

# Quantitative susceptibility mapping by regulating the field to source inverse problem with a sparse prior derived from the Maxwell Equation: validation and application to brain

J. Liu<sup>1</sup>, T. Liu<sup>2</sup>, L. de Rochefort<sup>3</sup>, I. Khalidov<sup>1</sup>, M. Prince<sup>1</sup>, and Y. Wang<sup>1,2</sup>

<sup>1</sup>Radiology, Weill Cornell Medical College, New York, NY, United States, <sup>2</sup>Biomedical Engineering, Cornell University, Ithaca, NY, United States, <sup>3</sup>MIRcen, I2BM, DSV, CEA, Fontenay-aux-roses, France

## INTRODUCTION

The field inhomogeneity mapped using MRI offers the opportunity to characterize tissue magnetic susceptibility. The field measured in a voxel is a dipole kernel convolution of all tissue susceptibility sources surrounding the voxel [1]. The zero cone surfaces of the dipole kernel in Fourier domain undersamples the measured field, causing ill-posedness for the inverse problem of deriving susceptibility source maps from the magnetic field [2,3]. However, if a proper prior could be found to sparsify the signal, even highly undersampled data may allow an exact reconstruction [4]. Here, we propose an approach for achieving quantitative susceptibility mapping (QSM) by exploiting the sparsity derived from Maxwell's equation and the  $T_2^*$  weighted image. Phantom experiments demonstrate artifact free and accurate susceptibility reconstruction. High quality QSM of human brain indicates the encouraging advances of QSM.

## MATERIALS AND METHODS

According to the magnetostatic Maxwell equation, the change of susceptibility causes magnetic field change, hence  $T_2^*$  decay and signal change in  $T_2^*$  weighted images. This provides insight into choosing proper prior knowledge: the susceptibility changes which are not reflected on  $T_2^*$  weighted images should be extremely sparse. With such a high sparsity, information theory suggests that there is an overwhelming probability to exactly recover the undersampled data [4].

In theory, optimum sparsity occurs with  $L_0$  minimization. Here we investigated two implementations, weighted  $L_1$  and homotopic  $L_0$  to approach solutions that approximate the optimal  $L_0$  solution [5,6]. The inverse problem may be formulated as  $\min_{\chi} |W_G G \chi|_L$ , s.t.  $|W(C\chi - b)|_2 < \epsilon$ , where  $\chi$  denotes susceptibility spatial distribution,  $b$  is the measured magnetic field,  $C$  a matrix representing the convolution kernel of the dipole,  $G$  is an operator such as the gradient operator that promotes sparsity,  $L$  is a choice of norms ( $L_1$  or  $L_0$ ), and  $\epsilon$  is the error.  $W$  weights the phase noise variation at each voxel and can be derived from MR image magnitude.  $W_G$  weights the large gradients of the image magnitude with zeros and the smaller gradients with ones. The minimization problem can be reformatted and solved efficiently with conjugate gradient method [5].

The proposed method was validated with phantom experiments: Gd doped water balloons with different known susceptibility values were imaged with a multi-echo gradient echo sequence on a 1.5T GE scanner; SPIO doped agarose gel phantom with different known amounts of iron was imaged at 3T GE scanner. The method was applied on healthy volunteers ( $n=7$ ) and patients ( $n=11$ ) with brain hemorrhages at 3T. Imaging parameters were: 3D axial gradient multi-echo sequence with flow compensation, FOV=24cm, slice thickness=2 mm, image matrix=240x240, BW=62.5KHz, TR/TE=40/5,10,15,20,25 ms, FA=20°. Phase unwrapping and effective dipole fitting background removal were applied to extract the field map. The brain region was segmented out for calculating QSM. The final solution to the minimization programming was chosen when the residual norm matched the expected noise norm  $\epsilon$  [7]. Iron concentrations were calculated by summing susceptibilities over a ROI and dividing by the volume.

## RESULTS AND DISCUSSION

Methods of  $W_G$  weighted homotopic  $L_0$  and  $L_1$  norm minimization provide comparable solutions that are close to optimum (Fig.1). The weighted  $L_1$  method is at least twice faster and is preferable. These two methods need further careful comparisons in the future. In the SPIO phantom (Fig.2), even though the signal void makes the field map unreliable, the proposed weighted  $L_1$  method accurately recovered the QSM. Iron concentrations precisely matched the expectations. QSM on patients with brain hemorrhages indicated bleedings extremely clearly (Fig.3). Additively, iron rich structures such as the substantia nigra and the red nuclei appeared uniformly paramagnetic (Fig.3-4). Susceptibilities were measured at different location and values of  $\sim 0.36$  ppm for veins,  $\sim 0.18$  ppm for globus pallidus,  $\sim 0.13$  ppm for substantia nigra and red nucleus were obtained. Iron measure in brain tissues, might be useful in characterizing hemorrhages, aging processes and neurodegenerative diseases.

## CONCLUSIONS

Our proposed sparsity optimization method has been validated by phantom experiments with high accuracy and good image quality. Brain QSM provides an enhanced visualization and valuable quantification of iron in the brain. Quantitative susceptibility mapping offers a new methodology to measure endogenous and exogenous susceptibility contrasts.

**REFERENCES:** 1. Marques JP, et al, CMR, 25, p65, 2005. 2. Liu T, et al, MRM, p196, 2009. 3. Kressler B, et al, IEEE TMI, 2009. 4. Donoho, DL, IEEE Info Theory, 52, p1289, 2006. 5. Trzasko J, et al, IEEE TMI, p106, 2009. 6. Candes, JE, et al, JFAA, p877, 2008. 7. Gonzalez RC, et al, Digital image processing, 1992.

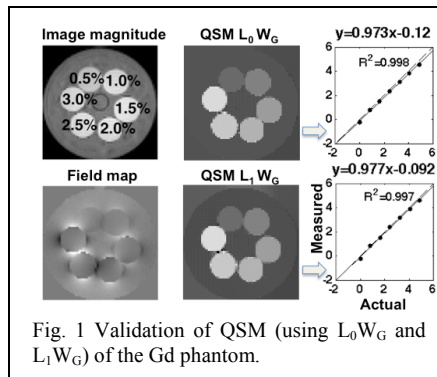


Fig. 1 Validation of QSM (using  $L_0 W_G$  and  $L_1 W_G$ ) of the Gd phantom.

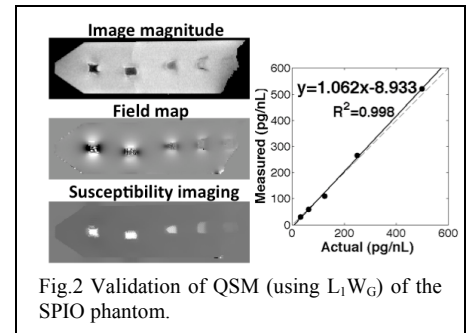


Fig.2 Validation of QSM (using  $L_1 W_G$ ) of the SPIO phantom.

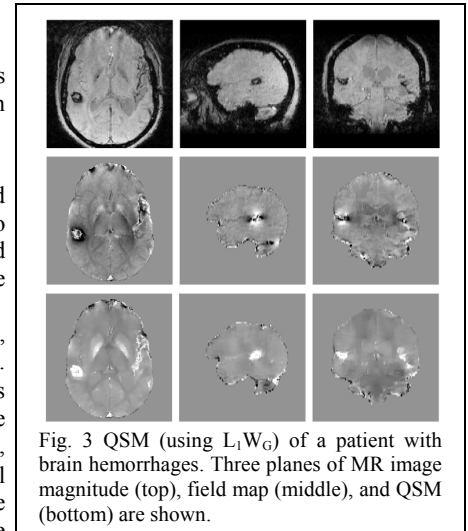


Fig. 3 QSM (using  $L_1 W_G$ ) of a patient with brain hemorrhages. Three planes of MR image magnitude (top), field map (middle), and QSM (bottom) are shown.

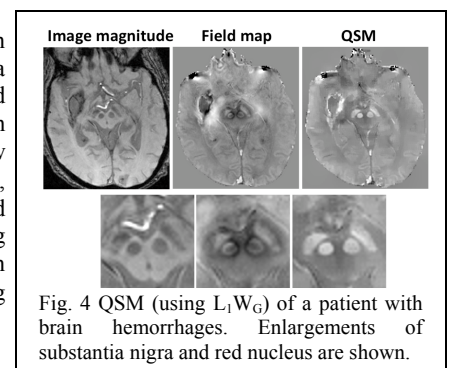


Fig. 4 QSM (using  $L_1 W_G$ ) of a patient with brain hemorrhages. Enlargements of substantia nigra and red nucleus are shown.